

Design and fabrication of a MEMS mirror for Miniature Laser Projection

René Sanders*, Diederik van Lierop, Boudewijn de Jong, Herman Soemers
Philips Applied Technologies, High Tech Campus 7, 5656AE, Eindhoven, Netherlands
[*rene.sanders@philips.com](mailto:rene.sanders@philips.com); Phone +31.(0)40.27.48722; Fax +31.(0)40.27.46366

ABSTRACT

For miniature laser projection displays the laser beam is swept very fast back and forth with a MEMS mirror. This paper presents an innovative design for such a MEMS mirror. Both the dynamical behavior and manufacturability have been improved. We designed a process based upon industrially proven process steps to accurately control critical parameters and fabricated a mirror consisting of: cantilever beams, out-of-plane support beams and a rhombus shaped enforcement structure.

Measurements show a well defined resonant mode of operation at 23.5 kHz while suffering from only little parasitic resonance modes. This mirror can now be mass-produced at low costs.

Keywords: MEMS mirror, laser display, pocket projector

1. INTRODUCTION

Small electronic devices such as mobile phones, PDA's, and multi-media players, are becoming increasingly more popular. Consumers can access and exchange information at any time at any place. Whereas these devices become smaller and at the same time the amount of information increases, there is a need for a new technology that is both small and at the same time can display a large amount of information in a convenient way. Miniature Laser Projection is one of the most promising technologies for this need¹.

One of the key components of laser projection systems is the scanning mirror for the fast back and forth sweeping of the laser-beam. As will be explained, the dynamic requirements for such a mirror are very challenging. To achieve an optimum *overall* design (i.e. excellent dynamic performance and to be manufactured at low cost, in high volumes with high yield) requires a truly multi-disciplinary approach by taking into account mechatronics, process technology, optics and system architecture.

2. DESIGN REQUIREMENTS AND CHALLENGES

For use in a hand held consumer product, the key drivers are: good image quality, small size, low power consumption and of course low cost. An excellent overview of the challenges these requirements have on the design is given elsewhere². Here, we want to recall some of their most relevant results and the consequences for our design.

2.1 Scan frequency, mirror diameter and scan angle

A simple metric for quality is resolution. As an example, take a SVGA (800x600 pixels) image. At a refresh rate of 60 Hz, the line frequency is $600 \times 60 = 36$ kHz. To achieve these high frequencies at low power consumption, the mirror needs to be operated in resonance mode. Typically the movement of the mirror then is sinusoidal: the forth movement being identical to the back-movement of the mirror. Therefore, using bi-directional scanning becomes very favorable and it halves the required scanning frequency. Because the information close to the turning points cannot be used, the resulting scanning frequency for the fast axis needs to be *at least* 18 kHz.

The resolution also determines the required number of resolvable spots. Independent of the details of the optical system, this number depends linearly on the product of the mechanical scan-angle and the diameter of the scanning mirror, θD , which must be larger than 10 [deg.mm]^{2,3,4}

The inertial forces at the turning point are very large due to the high operating frequency, which result in a significant dynamic deformation of the mirror. A larger mirror leads to a higher mass and higher moment of inertia. It can be shown that the deformation scales with the 5th power of the mirror diameter! As a rule of thumb, deformation of optical surfaces should be less than $\lambda/10$, or 50 nm, which limits the mirror diameter to typically a maximum of ϕ 1.5 [mm]. To obtain a high θD value it is therefore easier to increase the scan-angle (θ) than to increase the diameter (D), as long as the maximum stress level due to elastic deformation in the mirror's suspension is within limits (the mechanical stress is proportional with the scan angle).

On the other hand, a small mirror requires a more stringent opto-mechanical alignment of the optical components. On top of that, additional optical components might be required to image the laser beam onto a projection screen. Based upon some first-order calculations, the diameter of the mirror is selected to be ϕ 1.0 [mm]. This means that the mechanical scan-angle of the fast axis should be at least 10 degrees.

The slow axis for horizontal scanning has an operating frequency of 60 Hz. In principle the slow axis can also be operated in resonance mode. However, small position deviations now have consequences for a complete line. Especially for the case of bi-directional scanning of the slow-axis, the requirements for stability and accuracy are very high. Uni-directional scanning halves the duty-cycle and is therefore not an option. An alternative is to use direct drive mode instead and then apply a saw-tooth motion⁶. This however requires quite a powerful actuator considering the small dimensions!

The most important architectural design choice to be made is between a single mirror with two rotation axis (1x2D) and two individual mirrors each having a single rotation axis (2x1D). Obviously, the dual axis mirror is the Holy Grail because it requires the least silicon real-estate and because it saves an additional mirror, which reduces the alignment effort, volume claim, and optical losses^{7,10, 11, 13, 16}. At the same time it also has some drawbacks:

- The fast-axis is usually suspended in an intermediate body to create a gimbal suspension. This intermediate body adds compliance to the suspension, which will increase the amplitude of motions of the fast-axis other than the primary rotation. Additional parasitic resonances will be introduced because of the internal degrees-of-freedom of the intermediate body, which will have an adverse affect on the image quality.
- The intermediate body must be stiff (see the previous point), which adds mass to the slow axis and requires precious silicon real-estate. A 2D mirror, including a gimbal suspension and actuators, will therefore be typically 2½ x larger (in area) than a single 1D mirror, which limits the overall gain in silicon real-estate.
- Cross-talk will be much more prevalent because the two tilting axes are tightly integrated and will share parts of the suspension, and because the actuators are very close and might affect each other. It will therefore be quite a bit harder to achieve the required quality of the projected image!
- Both mirrors must be made in a single process, but the requirements with respect to the mechanics and actuation will be different due to the differences in operating frequency. This leads to additional compromises. Individual single-axis mirrors however can be optimized independently.
- A 2D resonant scanner using Lissajous projection mode requires dedicated image processing which might be a compatibility issue.

Our believe is that the added complexity of a 2D-mirror outweighs the gains. This is why we have decided to aim for a 2x1D architecture. This paper describes our work on the fast moving mirror.

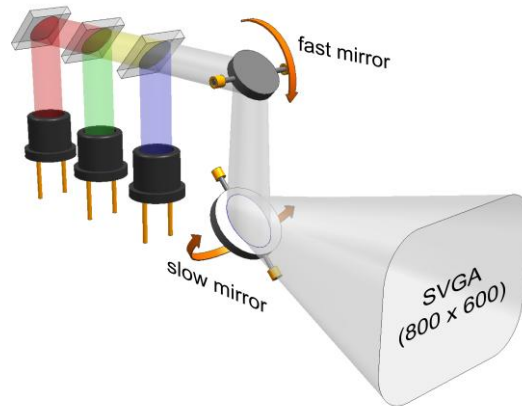


Fig. 1 Schematic of a 2x1D laser projection architecture

2.2 Actuation

The most suitable actuation principles demonstrated so far in MEMS scanners are electrostatic, electromagnetic, piezoelectric and thermal actuation. Thermal actuators¹⁹ are able to develop large forces but it is difficult to achieve high frequency operation, stability at frequencies such as those needed for high resolution imaging, and power consumption is very high.

Although the piezo-actuators are able to meet the requirements for high-frequency operation and develop significant forces, they have only a limited stroke. A lever mechanism is needed for greater displacement demands, which adds complexity and compliance (quadratically scaling with the transmission ratio). On top of that, processing of piezo-active layers significantly increases the cost and complexity of the manufacturing process¹⁸.

Disadvantages of the electromagnetic actuators with coils placed on the moveable part of the structure are the increase of the moveable mass, the thermal dissipation due to electrical losses in the coil, and additional stress and distortion of the micro-mirror flatness due to difference in the thermal expansion coefficient between the mirror body and the coil. Large forces can be developed if external permanent magnets are used which allows for a high accelerations⁶. Moveable permanent magnets would add mass to the mirror and increase the mirror deformation, partly due to possible differences in thermal expansion.

The possibility of batch processing of an electrostatic actuator makes it the preferred choice for MEMS scanners from a cost point of view. No additional external parts for assembling or materials that are difficult to process are needed. Thermal issues are negligible because power dissipation will be in the μWatt range and only 1 type of material is used. Scan angle can be very large, only limited by mechanical stress in the hinges¹⁵ and electrical breakdown in the comb fingers.

2.3 Mirror suspension

The human eye is very sensitive to image irregularities, distortions and jitter caused by the scanning device, which poses very strict requirements on the dynamic performance. Parasitic resonant modes occurring close to the frequency of the fundamental torsional mode must be avoided at all cost. This poses extra challenges on the suspension of the mirror. Any suspension constructed using elastic deformation of bulk material will have many different eigenmodes, see the examples for a torsion-beam suspended micro-mirror below. Especially worrisome is the rocking mode. Its rotation axis coincides with the rotation axis of the other (slow) scan angle. Due to the large distance of the mirror to the screen, even small tilting angles will quickly lead to significant displacement of the projected spot.

The other modes will not affect the image quality directly or only to a lesser extent. They will however influence the electrostatic comb-drive actuator because the overlap of the fingers and the gap in between those fingers will change, possibly leading to asymmetry, additional non-linearity, pull-in, or even electrical breakdown or mechanical damage! A well balanced dynamic behavior is therefore required.

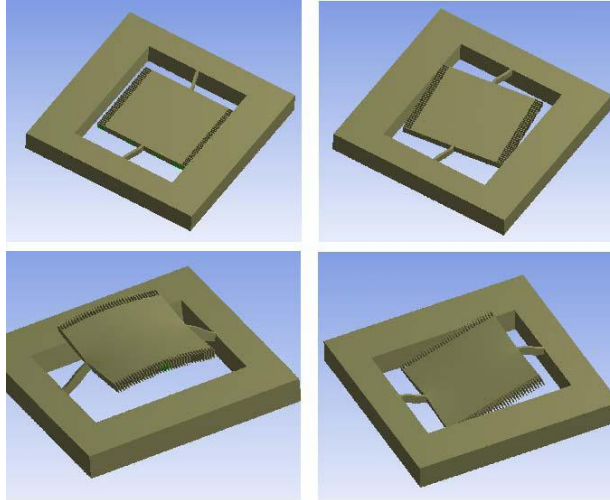


Figure 2: Parasitic resonance modes (2nd – 5th), only some of them having an effect on image quality.

Using only torsion beams it is difficult to control the dynamic behavior accurately, especially when going to high frequencies and large deflections. With such requirements one will end up with quite long and thick torsion beams, which not only require a large die size but are also not very effective in suppressing the parasitic eigenmodes: the torsion beams must provide both stiffness, to create an eigenfrequency and to suppress parasitic eigenmodes, and compliancy, to allow for a large scan angle.

2.4 Summary

The design needs to fulfill some conflicting requirements: minimal dynamic deformation of the mirror surface, while avoiding high mechanical stresses, having the largest possible scan angle and mirror diameter, requiring only little power, while avoiding parasitic resonant modes and of course to be manufactured at the lowest cost. From some first-order calculations we arrive at the following characteristics of a MEMS scanning mirror for miniature laser projection:

- diameter of the mirror is 1.0 [mm],
- mechanical scan angle is ± 10 degrees,
- scan frequency > 18 kHz,
- operated in resonance mode,
- electrostatic actuation.

3. MECHANICAL DESIGN

A general design rule to obtain the maximum bandwidth and accuracy in any dynamical mechanical design, is to design a light and stiff construction. Secondly, to create an exactly constrained mechanism where possible: any degree-of-freedom (DOF) should be constrained exactly once.

The class of mirror designs that comes closest to our requirements is known as a ‘torsion beam scanners’. The pair of torsion beams used in these devices should ideally provide a single rotational DOF with both:

- a large allowable strain to allow for a large tilt angle, and
- a well-defined but finite stiffness to provide an eigenfrequency, and
- an infinite stiffness in all five other DOFs to suppress unwanted rigid-body motions

Combining these contradicting requirements into a single pair of beams leads to compromises, at the cost of the dynamical performance of the device. The solution is found in separating stiffness from suspension: we use four

cantilever beams to provide a well-defined stiffness around a single rotation axis. This rotation axis is defined by two thin and short torsion beams, as depicted below. These torsion beams have a negligible torsional stiffness when compared to the stiffness provided by the cantilever beams, which can be realized by making them relatively thin (in X -direction). At the same time they can have sufficient height (in Z -direction) and can be kept short (in Y -direction), resulting in an excellent out-of-plane stiffness. This nicely suppresses the out-of-plane translation mode T_z and rocking mode R_x , which are the two most important parasitic modes from an optical engineer's perspective. This would not have been possible if the torsion beams had to provide the torsional stiffness too!

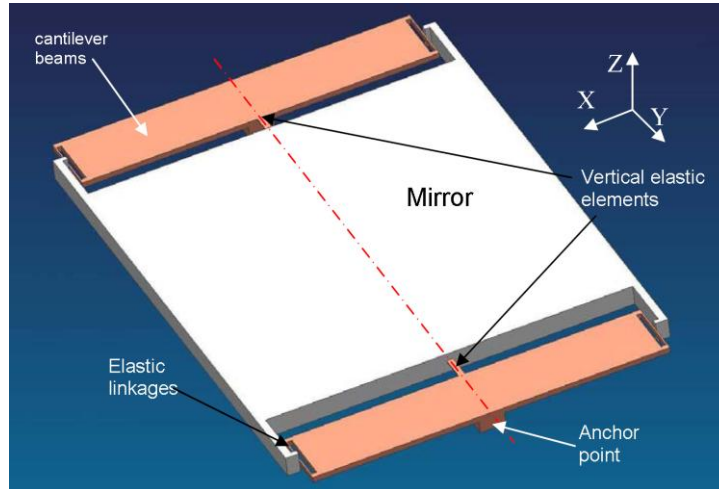


Figure 3: Schematic of the mirror design.

Others have demonstrated honeycomb structures below their mirror which reduces both mass and stiffness if the thickness of the mirror stays the same⁸. Although this is not useful to reduce the dynamic deformation, this might still be useful to increase the eigenfrequency of the fundamental mode due to the lower inertia. When a honeycomb structure is used to increase the thickness of the mirror body without increasing its mass however, then this will definitely reduce the dynamic deformation. Still, most of the body will not be used very efficiently when looking at the mechanical energy density. The material near the rotation axis will be more heavily loaded than the material at a larger distance because the bending moment due to the inertia forces is higher. The biggest contribution to the mirror stiffness will therefore be supplied by material near the rotation axis, and material at the outer edges can safely be removed. This obviously has a strong effect on the inertia, and therefore reduces the dynamic deformation. This effect has been utilized by Ji et. al.⁹, who reinforced their mirror using multiple parallel beams, each beam individually shaped as a parallelogram. Using parallel beams like that though will yield a mirror body with an internal DOF, because these beams can still rotate with respect to each other. Torque exerted on the mirror by the torsion beams (or by the cantilever beams in our design) has to be transferred to the middle of the mirror, for which a rigid body is needed. To this end we have designed the beams in our supporting structure in an “XX” arrangement, as depicted below in figure 4b. This eliminates the internal DOF and therefore reduces the dynamic deformation even further. When oscillating at high frequencies, the two points where the X's intersect will be lagging with respect to the points where cantilever beams are connected to the comb-drive. The deformation of the mirror surface in our design due to this effect has been calculated using FEM and has been depicted in figure 5b. The supporting beams in the “XX” arrangement nicely connect the deformation peaks with each other, just as they do for the deformation valleys. Using this design a diffraction-limited spot can be achieved (which will be discussed in more detail at the end of this chapter). A subsequent improvement could be to introduce a honeycomb structure in these supporting beams to increase their thickness without adding additional inertia, but we do not yet see a strong need for that.

An additional benefit of this arrangement with cantilever beams and stiff supporting structure is that the mirror is excited at its four corners where the largest contribution to the moment of inertia is located, as opposed to the more common designs in which the mirror is excited close to the rotation axis. This reduces the bending moment throughout the mirror. Closely related to that, the width of the comb-drive can be chosen independently from the mirror diameter (to some

extent). Finally, the comb-drive has been rigidly connected to both the supporting structure and the cantilever beams using a reinforcement beam, which reduces the dynamic mirror deformation.

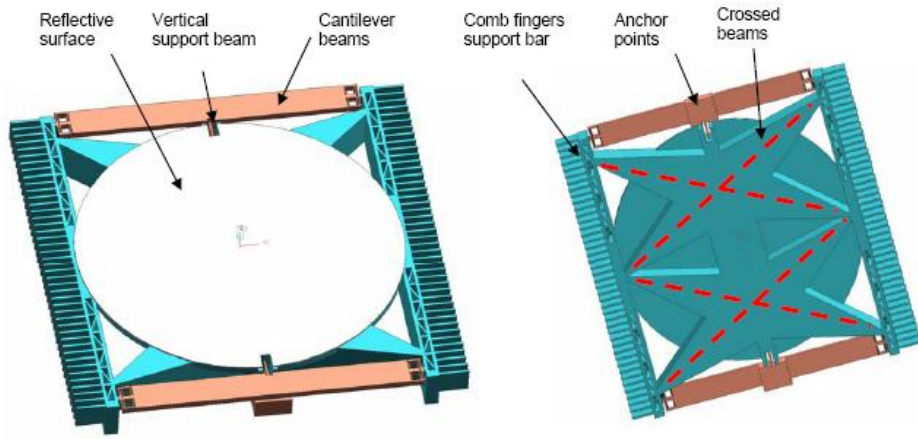


Figure 4: Mechanical design of the cantilever beam scanner a) top-view b) bottom view

A detailed analysis has been performed to assess the performance of this design, including:

- first-order analytical calculation of the stresses and frequencies of the eigenmodes
- static and dynamic FEM analysis to verify these analytical calculations
- FEM calculations of the dynamical deformation of the mirror surface
- analysis of the effect of the mirror deformation on the spot quality, using raytracing software
- estimation of the damping using published results of other comparable micro-mirrors
- FEM calculations of the capacitance of the actuator
- modeling of the dynamics of the mirror and the non-linear actuator including feedback control, using model-based design tools

In fig. 5a the calculated capacitance per finger is given as a function of mirror angle. Since the actuating force scales with capacity, it follows that the actuator is strongly non-linear²⁰. Fig. 5b gives the result for the calculated maximum deformation of the mirror surface at maximum scan angle. The calculated surface deformation is ± 40 nm.

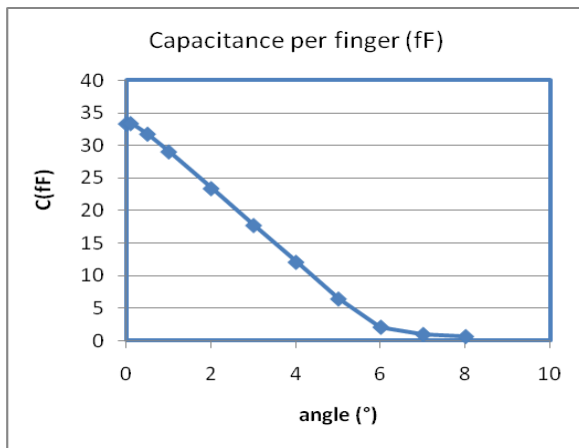
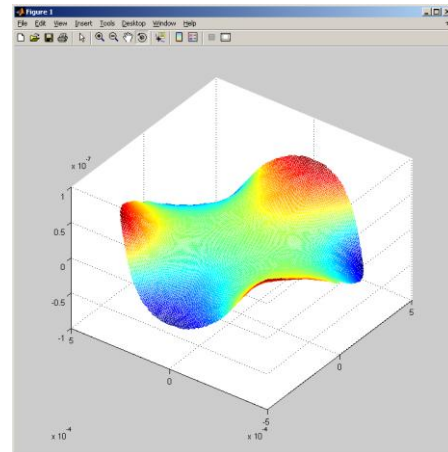


Figure 5(a) calculated capacitance per finger



5 (b) mirror shape used as input for optical analysis

To assess in more detail the consequences of the mirror deformation, the calculated surface is used as an input for optical raytracing. In our ray-tracing model, we ‘illuminate’ the MEMS mirror at 45° with a $\phi 0.6$ [mm] beam. In Figure 6b we show the spot diagram after reflection on the MEMS mirror at a distance of 1 [m]. The three-fold symmetry of the mirror is also visible in the spot shape. So how bad is this? The optical quality of the mirror can be expressed in terms of optical path difference. For this, we included a 100 [mm] focal-length, aberration-free paraxial lens. The RMS OPD is 14 m λ , the peak-to-valley OPD is 85 m λ which corresponds to a Strehl ratio of 99.3 %. A generally accepted maximum level of aberrations, so that the spot can still be considered diffraction-limited is 80 m λ RMS OPD (Strehl ratio 80%). As the RMS OPD is below the diffraction limit, the diffraction will be dominant in the spot size which indicates that the effect of the dynamic mirror deformation is indeed negligible.

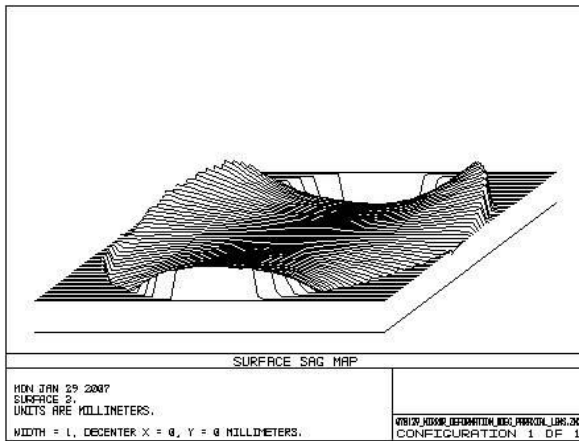
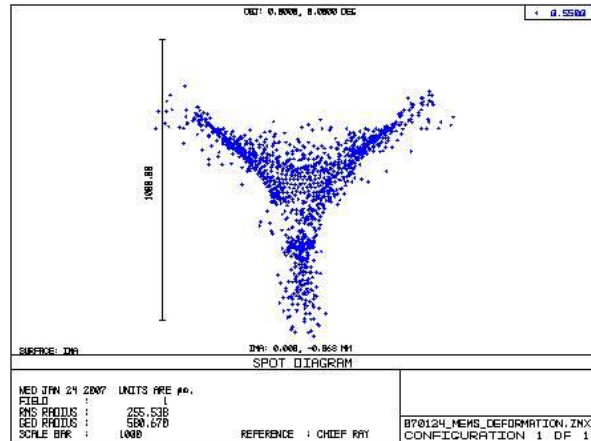


Fig.6a Deformed mirror surface as input for raytracing



6b. Calculated beam intensity distribution at 1 m distance

All results of simulations are summarized in the table below:

Parameter	Unit	Basic analytical calculation	FEM
Fundamental mode	[kHz]	18.6	18.8
In plane translation	[kHz]		45
In plane rotation	[kHz]		76
Out-of-plane translation	[kHz]	279	144
Out-of-plane rotation (rocking)	[kHz]	519	255
Quality factor (in air)	[-]	200	
Driving voltage at 7.4°	[V]	60	
Mirror surface deformation	[nm]	± 40	
Energy injected per cycle	[J]	2×10^{-7}	

Table 1. Summary of calculated values of the cantilever beam scanner

4. MANUFACTURING THE MIRROR

Essential items of the mirror are: resonance frequency and maximum scan angle. The most critical characteristics that determine these items are the stiffness of the torsion beam and the size and weight of the mirror.

The cantilever beams provide their stiffness by bending. This stiffness is proportional to the third power of the thickness, which therefore has to be defined very accurately. For this purpose our design utilizes the device layer of an SOI wafer, of which the thickness can be controlled very accurately. Lateral dimensions are determined by lithography, alignment accuracy and etch properties (especially for the back side). By proper adjustment of the process parameters these can be controlled sufficiently accurate. Height and thicknesses are typically defined by etching time. However, since etching rate depends on the aspect ratio of a feature an extra process step is needed to accurately define critical height dimensions. This is the use of a BOX (Burried Oxide) layer at a well defined height position, that acts as an etch stop layer.

Other important mechanical feature are elastic linkages in between the cantilever beams and the mirror, which are compliant in X direction but stiff in Z-direction. This is needed because the cantilever beams will bend, whereas the mirror only tilts without any static deformation. The elastic linkage will overcome the resulting difference in length by expanding in X-direction.

In general, the torsion beam suspended devices are fabricated device layer of a SOI wafers. Unlike these fabrication approaches, our design requires fabrication in both top and bottom Si layers of the wafer. Top and bottom DRIE (Deep Reactive Ion Etch) steps are used to define the required height features.

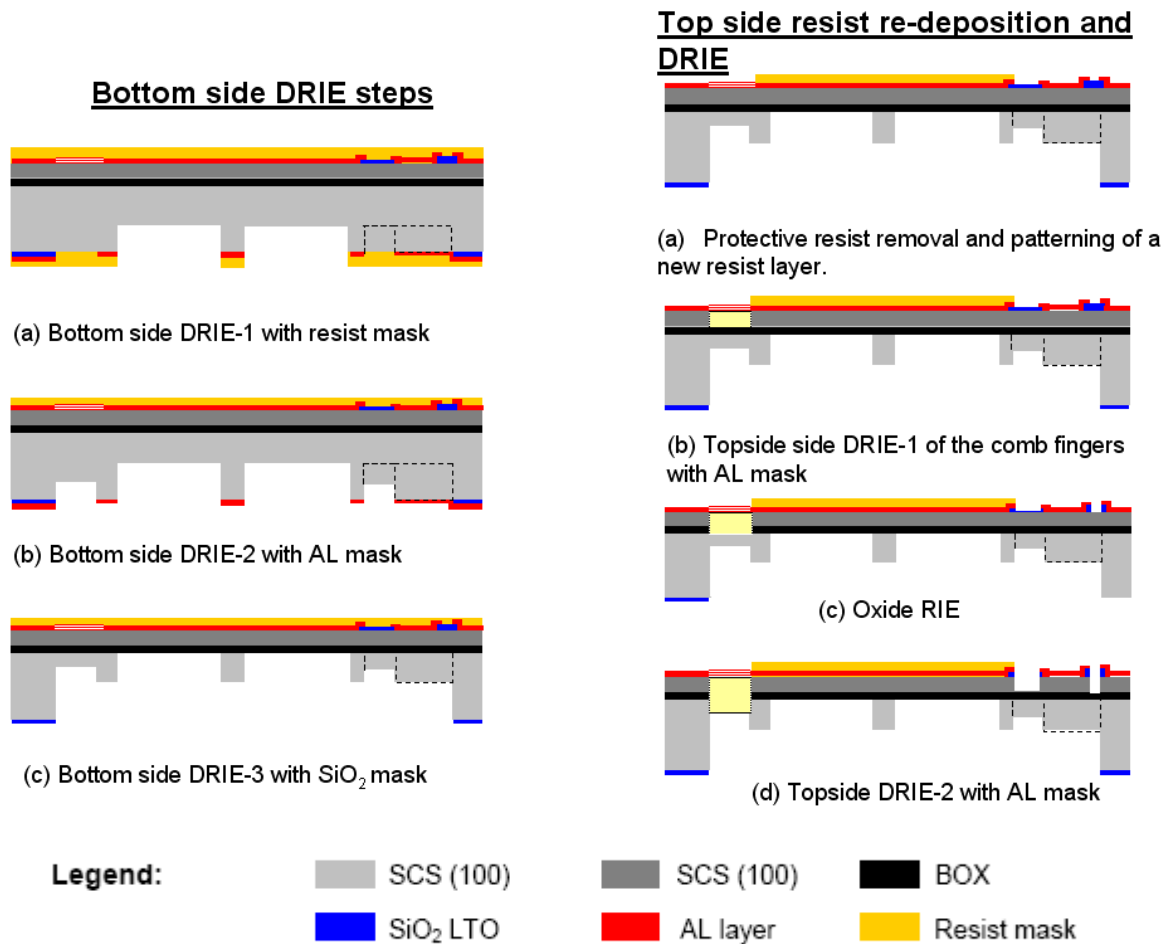


Fig.7: Schematic process flow for the manufacturing of the Apptech mirror

The BOX layer divides the whole device in a top and bottom layer. Next to this, because the mirror part needs to be electrically isolated from the fixed world, center and outer parts of the device are electrically isolated. This adds up in 4 separate potential areas:

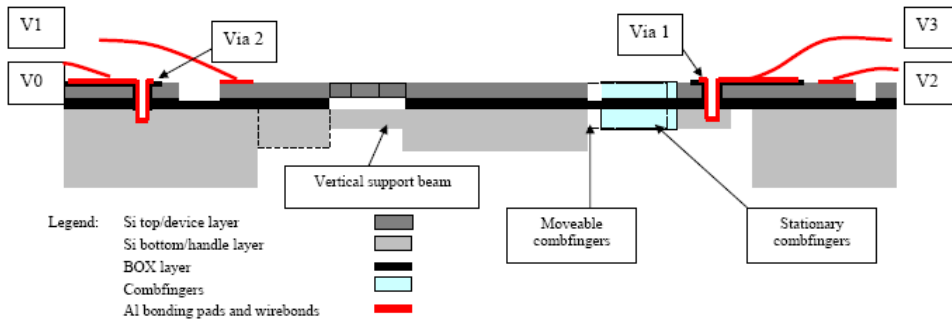


Fig.8 Schematic cross section of the mirror with the 6 separate potential areas.

For redundancy purpose, all connections are duplicated. That means that we have in total 12 electrical connections to the device. All contact pads are located at the top side of the device. Electrical contact to the outside world is done by wire-bonding. To minimize the risk of having no functional devices after processing, we simultaneously processed 4 design-variations. Each design contains a step-wise increase in detail and complexity, while at the same time having the basic functionality.

A pre-requisite for mass manufacturing is the ability to transfer the mechanical and process design to a MEMS foundry. After finalizing the mechanical design and associated process flow, a suitable MEMS foundry was selected and found: Silex Microsystems²³. The results described in the following chapter prove that the transfer was successful.

5. RESULTS AND MEASUREMENTS

Out of the first processed batch, there were 54 useable dies. Other dies were rejected because of insufficient etching of the comb-fingers, breakage of fragile parts or breakage during handling. Typical SEM-images of useable dies are given in fig.9. The relevant features are according to specification and can be compared with the design (fig.3):

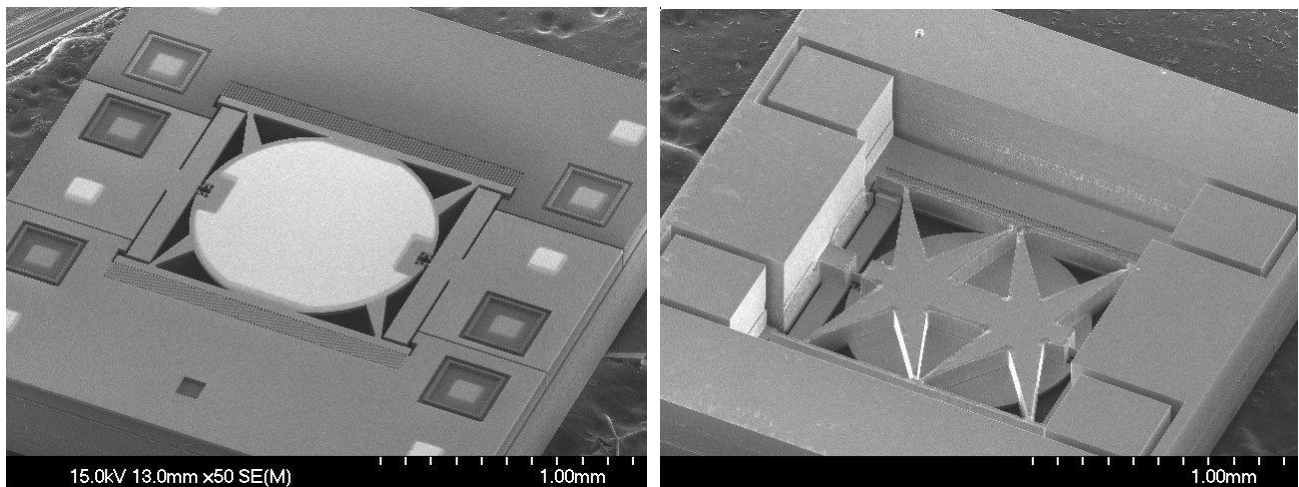


Fig.9. SEM images of processed mirrors. A) Top-side. B) Bottom-side.

The accuracy of the processed dimensions is very good, as can be seen from table 2 containing measurement data of some characteristic dimensions of fabricated mirrors:

Thickness 1	Thickness 2	Bar	Comb finger	Pitch comb
-	-	-	3.8	7.1
42	95	20.6	3.6	7.0
34	87	21.0	3.8	7.1
36	84	20.7	3.7	7.1
41	85	20.1	3.5	6.9
38	83	20.5	3.6	6.9
37	88	21.4	3.5	7.0

Table 2 Measurements of thicknesses and dimensions of the com-fingers (data in microns)

The next picture shows the wire-bonded mirror glued onto a PCB:

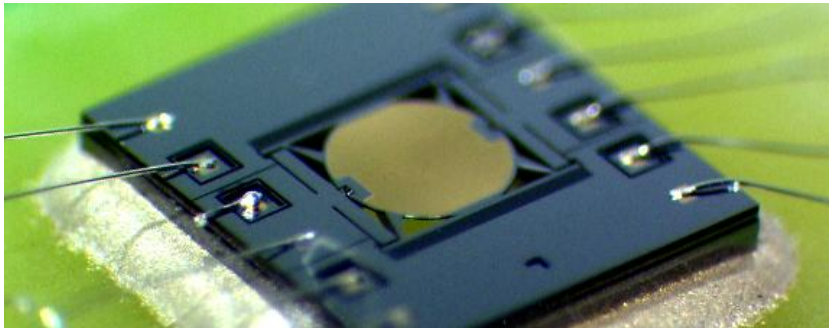


Fig.10 Photograph of a mounted and wire-bonded mirror

The flatness of the mirror surface is within 40 nm as indicated by a Veeco interferometer measurement:

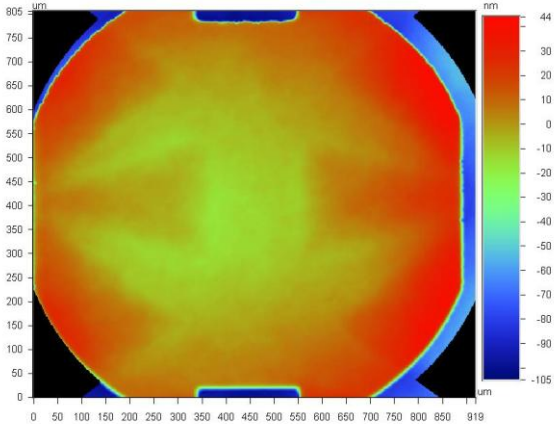


Fig.11 Flatness measurement of the mirror surface

The dynamical properties of the mirror have been characterized using a Polytec MSA laser vibrometer²⁴. To find as many eigenmodes as possible we have mounted the device on a piezo shaker (electrical actuation using the comb-drive actuator only revealed the fundamental mode with an otherwise very clean spectrum).

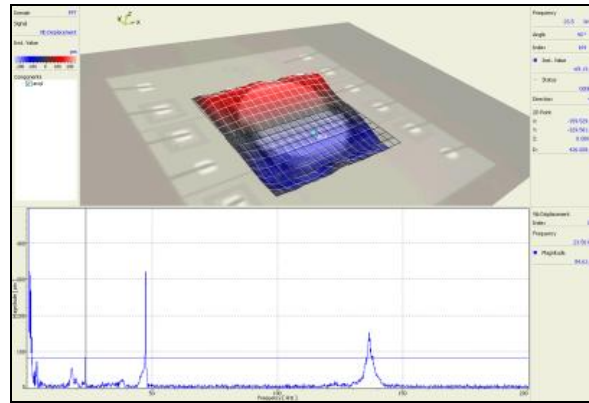


Fig.12 Characterization of dynamical properties using a Laser Vibrometer

The measurements show very well defined resonance peaks at 23.5 kHz and 47 kHz, being the fundamental mode and its second harmonic. All mirrors exhibit all well defined resonance in the range of 23.3-23.6 kHz. These are different from the design value (18.6 kHz) probably because the oxide layer has not been removed from the cantilevers.

The resonance observed a bit below 20 kHz can be contributed to eigenmodes of the PCB (cross checked by measuring a bare PCB without a mirror). The other resonance peak at 137 kHz is from the out-of-plane translational mode. The in-plane dynamic modes, which are to be expected in between the frequencies mentioned above, cannot be measured because these do not result in a Doppler shift.

We have build a very simple setup using a wave-form generator, a laser source and a PSD (Position Sensitive Detector) to enable characterization of the actuator and mirror in open-loop operation. The setup is PC-controlled using Labview for automated data-acquisition and analysis. In the graph below you will find a typical measurement result of the scan-angle as a function of both the frequency and excitation voltage, in which both frequency and voltage are varied in up- and down-ward direction (varying only one parameter at a time, while keeping the other constant). The asymmetry in the frequency response is caused by the non-linear behavior of a comb-drive actuator²⁰:

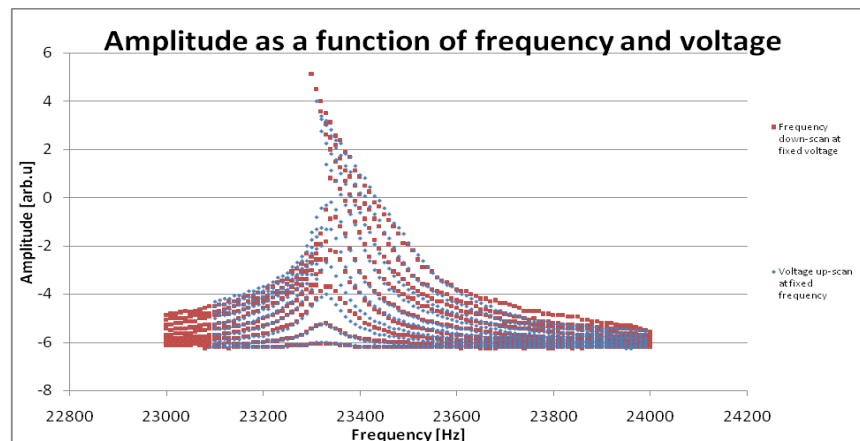


Fig.13 Scan angle as a function of frequency and voltage.

Currently we are testing our device in closed-loop operation, using a phase-locked-loop. Results of this will be published later this year.

6. SUMMARY AND CONCLUSIONS

We motivated the use of a 2x1D mirror architecture for use in a miniature laser projector. Using basic design principles from traditional mechanical engineering we proposed a new scanner design based upon the decoupling of suspension from stiffness. On top of that, stiffness is enhanced by adding a rhombus shaped support to the mirror.

Simulations and measurements on fabricated devices confirm a lower deformation and improved suppression of parasitic eigenmodes. So far this device has proven to be very robust, although failure mechanisms have not been investigated yet and life-time performance analysis has still to be started.

The resonance frequency of fabricated devices is in the range of 23.3-23.6 kHz and differs significantly from our design value 18.6 kHz probably because the oxide layer has not been removed from the cantilevers.

Mass manufacturing capability has been shown by the successful transfer of our design to a MEMS foundry. Because the mirror can be fully batch manufactured and real-estate per mirror can be further reduced, the cost down result at high volume production is ensured.

7. ACKNOWLEDGEMENTS

This work has been sponsored in part by the Dutch government within the framework MEMSland.

The authors want to thank Silex Microsystems for fabricating the devices and our colleagues: Dr.M.Viegers for his long-term support; Krassimir Krastev, Toon Kuijpers, Eric van Kempen and Jorrit de Vries for all their valuable contributions.

REFERENCES

- [1] Y.Park et.al., “*Perspective of MEMS based raster scanning display and its requirements for success*”, Proc. SPIE vol 6114 (2006).
- [2] Hakan Urey and David Dickensheets, *Display and Imaging Systems*, Ch. 8 in MOEMS and Applications, E. Motamedi, Editor, SPIE Press (2005)
- [3] Hakan Urey, “*MEMS Scanners for Display and Imaging Applications*”, Proc. of SPIE Vol. 5604 (2004)
- [4] Hakan Urey, “*Torsional Scanner Design for high-resolution display systems*”, Optical Scanning II, Proc SPEI vol 4773, pp27-37 (2002)
- [5] Schenk H, Dürr P, Kunze D, Kück H, “*A new driving principle for micromechanical torsional actuators*”, Micro-electro-mechanical systems (MEMS) 1999., New York, NY: American Society of Mechanical Engineers, 1999, vol. 1 pp. 333-338
- [6] Arda D. Yalcinkaya, Hakan Urey, Dean Brown, Tom Montague, Randy Sprague, “*Two-Axis Electromagnetic Microscanner for High Resolution Displays*”, JOURNAL OF MICROELECTROMECHANICAL SYSTEMS, VOL. 15, NO. 4, AUGUST 2006
- [7] H.Schenk, “*A resonantly excited 2D-micro-scanning-mirror with large deflection*”, Sensors and Actuators A 89 (2001) 104-111
- [8] S.-T. Hsu, T. Klose, C. Drabe, A. Wolter, and H. Schenk, “*Ultra flat high resolution microscanners,*” in Optical MEMS and Nanophotonics, 2007 IEEE/LEOS International Conference on, pp. 197–198, Aug. 12 2007-July 16 2007.
- [9] Chang-Hyeon Ji et.al. “*An electrostatic scanning micromirror with diaphragm mirror plate and diamond-shaped reinforcement frame*”, J. Micromech. Microeng. **16** (2006) 1033–1039
- [10] A.Wolter et.al., “*Scanning 2D micromirror with enhanced flatness at high frequency*” Proc. Of SPIE vol.6114 (2006)
- [11] K.Roscher, “*Low-cost projection device with a 2D resonant microscanning mirror*” Proc. SPIE Vol. 5348 (2004) p.22-31
- [12] Young-Chul Ko et.al., “*Eye-type scanning mirror with dual vertical combs for laser display*”, Sensors and Actuators A 126 (2006) 218–226
- [13] Shu-Ting Hsu et.al. “*Two dimensional microscanners with large horizontal-vertical scanning frequency ratio for high resolution laser projectors*”, Proc. of SPIE Vol. 6887 (2008)
- [14] Il Woong Jung et.al. “*High Fill-Factor Two-Axis Gimbaled Tip-Tilt-Piston Micromirror Array Actuated by Self-Aligned Vertical Electrostatic Combdriives*”, JOURNAL OF MICROELECTROMECHANICAL SYSTEMS, VOL. 15, NO. 3, JUNE 2006
- [15] A. Wolter, “*Torsional stress, fatigue and fracture strength in silicon hinges of a micro scanning mirror*”, Reliability, Testing, and Characterization of MEMS/MOEMS III, Proceedings of SPIE Vol. 5343 (2004)
- [16] Ulrich Hofmann, “*Wafer-level vacuum packaged micro-scanning mirrors for compact laser projection displays*”, SPIE Proc. Vol. 6887 (2008)
- [17] Gary K. Fedder, “*Technologies for Cofabricating MEMS and Electronics*”, Proceedings of the IEEE | Vol. 96, No. 2, February 2008
- [18] Xiao-Hui Xu, Bao-Qing Li, Yan Feng and Jia-Ru Chu, “*Design, fabrication and characterization of a bulk-PZT-actuated MEMS deformable mirror*”, J. Micromech. Microeng. **17** (2007) 2439–2446
- [19] Ankur Jain, “*A Two-Axis Electrothermal Micromirror for Endoscopic Optical Coherence Tomography*”, IEEE JOURNAL OF SELECTED TOPICS IN QUANTUM ELECTRONICS, VOL. 10, NO. 3, MAY/JUNE 2004
- [20] Caglar Ataman, “*Nonlinear Frequency Response of Comb-Driven Microscanners*”, MOEMS Display and Imaging Systems II”, Proc.SPIE Vol.5348(2004)
- [21] Mita M, Mita Y, Toshiyoshi H, “*Multiple height microstructures fabricated by ICP-RIE and Embedded Masking layers*”, http://www.iee.or.jp/trans/pdf/2000/0011E_493.pdf
- [22] Madou Mark J., “*Fundamentals of Microfabrication*”, Second Edition, CRC Press, 2002
- [23] <http://www.silexmicrosystems.com>
- [24] <http://www.polytec.com>